Optimality of Contraction-Driven Crawling

P. Recho,[1,2] J.-F. Joanny,[1,3] and L. Truskinovsky[2]
[1]Institut Curie Centre de recherche (CNRS UMR168, UPMC, PSL Research University), 26 rue d'Ulm 75248 Paris Cedex 05, France
[2]LMS, CNRS-UMR 7649, Ecole Polytechnique, Route de Saclay, 91128 Palaiseau, France
[3]Ecole Superieure de Physique et de Chimie Industrielles de la Ville de Paris—ParisTech, 75005 Paris, France
(Received 3 February 2014; published 30 May 2014)

We study a particular mechanism of cell motility allowing a precise formulation of the condition of optimal trade-off between performance and metabolic cost. In the model, a steadily crawling fragment is represented by a layer of active gel placed on a frictional surface and driven by contraction only. We find analytically the distribution of contractile elements (pullers) ensuring that the efficiency of self-propulsion is maximal. We then show that natural assumptions about advection and diffusion of pullers produce a distribution that is remarkably close to the optimal one and is qualitatively similar to the one observed in experiments on fish keratocytes.

DOI: 10.1103/PhysRevLett.112.218101 PACS numbers: 87.16.Uv, 87.10.Ca, 87.16.Ln, 89.75.Kd

Although the idea of optimal trade-offs in biology is rather natural, the examples supporting optimality at the quantitative level are few. A prominent case is the demonstration that the structure of transport networks minimizes energy consumption at a fixed material cost [1]. Each validation of this type is of considerable interest as a step towards the general understanding of homeostasis [2–4]. In this Letter, we present a new example of cost-performance trade-off associated with contraction-driven cell motility. We observe that the distribution of molecular motors in crawling fish keratocytes [5] is similar to the optimal one and explain the physical mechanism leading to optimality.

The efficiency of self-propulsion in viscous environments has been a subject of intense studies since the pioneering work of Taylor [6]. Optimal strategies for various Stokes swimmers were identified under a tacit assumption that the organism is able to perform the desired shape changes [7,8]. Similar reasoning has been applied to crawling on frictional surfaces where the optimal propulsion can be induced by actuators prescribing spatially and temporarily correlated compression and stretch [9]. Such an approach, however, does not reveal the physical mechanisms ensuring optimal actuation, and it remains unclear whether actual cells can follow the optimal strategy.

To address these questions, we choose the simplest case of keratocytes whose motility initiation is largely contraction driven. Experiments show that contractile elements ("pullers") are narrowly localized at the trailing edge [5,10,11], and our goal will be to check whether such a configuration is optimal in terms of the trade-off between the Stokes performance and the energetic cost of active force generation and whether it is compatible with a minimal physical model. In our analysis, we neglect the presence of "pushers" because active treadmilling does not play an important role at the stage of motility initiation [12,13]. Several comprehensive computational studies of crawling taking treadmilling into account but not addressing the question of optimality are available in the literature [14].

We model a steadily crawling cell fragment using a one-dimensional version of the active gel theory [10,15–17]. The cytoskeleton is interpreted as an infinitely compressible viscous fluid, adhesion is represented by a frictional interaction with a rigid substrate, and the cortex is assumed to impose a fixed size on the moving cell. Using these simplifying assumptions and choosing parameters in the biological range, we show that the stationary distribution of motors is close to the optimal one.

Consider a one-dimensional layer of active gel placed on a frictional rigid background [15,16]. The balance of forces takes the form

$$\partial_x \sigma = \xi v,$$

where $\sigma(x,t)$ is the stress, $v(x,t)$ is the velocity, and ξ is the friction coefficient. We model the gel as a viscous fluid subjected to active contractile stresses $\tau(x,t) \geq 0$. We can then write

$$\sigma = \eta \partial_x v + \tau,$$

where η denotes the viscosity.

The regime of interest is when the cell moves with a constant velocity V while maintaining a length L fixed by the cortex. We, therefore, look for the configuration $\sigma(y)$ and $v(y)$ depending on the moving coordinate $y = (x - Vt)/L$ and satisfying the boundary conditions $v(\pm 1/2) = V$ and $\sigma(\pm 1/2) = \sigma_0$, where σ_0 is the reaction stress due to the length constraint. Without loss of generality, we assume $V \geq 0$.

The task is to find the distribution of active stresses $\tau(y)$ ensuring optimal efficiency

$$\Lambda = P/H,$$

where P is the functional power, and H is the metabolic cost per unit time. In the absence of an explicit cargo, we assume that the useful work is the translocation of the cell as a whole against frictional resistance. Therefore, we write

$$P = \xi V^2 L,$$

as in the theory of Stokes swimmers [18]. The rate of free energy consumption can be written as a sum $H = H^* + H^{**}$ where

$$H^* = -\int_{-1/2}^{1/2} \tau \partial_y v dy$$

is the power exerted by the active stress $\tau(y)$ on the environment, and H^{**} is the cost of the maintenance of the force generating machinery [19].

First, we suppose that the physical mechanism of force generation is unknown and pose the problem of finding the function $\tau(y) \geq 0$ maximizing Λ at a given value of H^{**}. We also prescribe the average value of the contractile stress

$$\bar{\tau} = \int_{-1/2}^{1/2} \tau(y) dy, \tag{1}$$

which is equivalent to fixing the total number of motors given the constant cell length. It will be convenient to use nondimensional variables $\sigma/\bar{\tau}$, $x/\sqrt{\eta/\xi}$, and $t/(\eta/\bar{\tau})$ without changing the notations. In dimensionless variables, the stress distribution can be written as

$$\sigma(y) = \sigma_0 \frac{\cosh(\mathcal{L}y)}{\cosh(\mathcal{L}/2)} + \mathcal{L} \int_{-1/2}^{1/2} \Psi(z,y)\tau(z) dz, \tag{2}$$

where

$$\Psi = \frac{\sinh[\mathcal{L}(\frac{1}{2}-y)]\sinh[\mathcal{L}(\frac{1}{2}+z)]}{\sinh(\mathcal{L})} - \theta(z-y)\sinh[\mathcal{L}(z-y)],$$

θ is the Heaviside function, and $\mathcal{L} = L\sqrt{\xi/\eta}$ is a parameter. The constants V and σ_0 can be found explicitly (cf. Ref. [12])

$$V = -\frac{\mathcal{L}}{2}\int_{-\frac{1}{2}}^{\frac{1}{2}} \frac{\sinh(\mathcal{L}y)}{\sinh(\frac{\mathcal{L}}{2})} \Delta\tau dy,$$
$$\sigma_0 - \bar{\sigma}_0 = \frac{\mathcal{L}}{2}\int_{-\frac{1}{2}}^{\frac{1}{2}} \frac{\cosh(\mathcal{L}y)}{\sinh(\frac{\mathcal{L}}{2})} \Delta\tau dy, \tag{3}$$

where $\Delta\tau = \tau(y) - 1$ is the spatially inhomogeneous component of the distribution of active dipoles, and $\bar{\sigma}_0 = 1$ is the prestress induced by its homogeneous component. The first of these formulas states that contraction-induced crawling is due entirely to spatial asymmetry: this is an analog of the famous scallop theorem [20]. Since the total force dipole produced by the system is $\mathcal{L}\int_{-1/2}^{1/2} yv(y)dy = \sigma_0 - \bar{\sigma}_0$, the second formula in Eq. (3) states that the inhomogeneity of motor distribution is also at the origin of a force dipole applied by the cell to the background [21]. Using Refs. [5,15,16,22], we obtain $\bar{\tau} \sim 10^3$ Pa, $\xi \sim 2\times 10^{16}$ Pam^{-2}s, $\eta \sim 10^5$ Pas, and $L \sim 20\times 10^{-6}$ m, which gives $\mathcal{L} \sim 10$.

The optimal distribution $\tau(y)$ depends on the parameter $\mathcal{H}^{**} = H^{**}\sqrt{\eta\xi}/\bar{\tau}^2$, which contains condensed information about the mechanism of active force generation. Optimality here implies a trade-off between maximization of velocity V and minimization of the power of active stresses $\mathcal{H}^*$. It is easy to show from Eq. (3) that the maximum velocity is $V^\infty = \mathcal{L}/2$ and that it corresponds to full localization of motors at the trailing edge. Similarly, one can reach the lower bound of the cost $\mathcal{H}^* = 0$ by taking $\tau = 1$; however, in this case, $V = 0$. The optimal trade-off depends on the value of $\mathcal{H}^{**}$, and it is clear that optimally distributed motors localize at $\mathcal{H}^{**} \to \infty$ and spread at $\mathcal{H}^{**} = 0$.

Mathematically, we have to solve an "obstacle" problem for a quadratic functional. Its solution has the form $\tau(y) = f(y)\theta(f(y))$, where $f(y) = Ay^2 + By + C$, and the constants A, B, C can be found from a simple algebraic minimization problem [23]. In the limit $\mathcal{H}^{**} \to 0$, we obtain $\Lambda \to (\mathcal{L}/2)\coth(\mathcal{L}/2) - 1$ and $\tau(y) \to 1 - 2y$. In the opposite limit $\mathcal{H}^{**} \to \infty$, the efficiency tends to zero as $\Lambda \sim \mathcal{L}(V^\infty)^2/\mathcal{H}^{**}$ and $\tau(y) \to \delta(y + 1/2)$, where δ is the Dirac distribution. In Fig. 1, we show the optimal efficiency $\Lambda_{\rm op}$ and some optimal profiles $\tau_{\rm op}(y)$ for intermediate values of $\mathcal{H}^{**}$. The regimes representing physical "designs" must be inside the admissible region bounded by the optimal curve $\Lambda_{\rm op}(\mathcal{H}^{**})$. Observe that under an alternative assumption $\tau(y) \leq 0$, we would have obtained exactly the same localization of *pushers* near the front end of the moving cell.

Suppose now that the active stress is generated by motors with mass density $\rho(x,t)$ and that $\tau = \chi\rho$, where χ is a positive constant. Following Refs. [10,24], we assume that

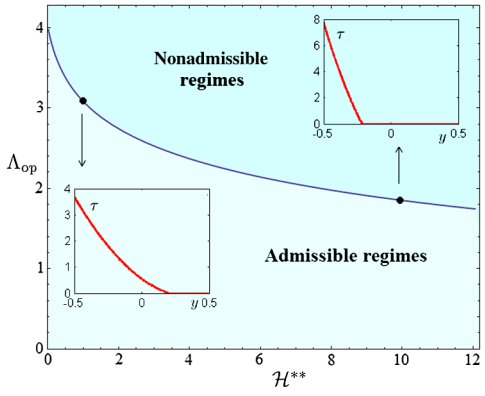

FIG. 1 (color online). Optimal efficiency as a function of the nonmechanical cost $\mathcal{H}^{**}$. The lighter colored zone represents the admissible region and inserts show optimal configurations. Parameter $\mathcal{L} = 10$.

the transport of motors is governed by the standard advection-diffusion equation, which in dimensional variables takes the form

$$\partial_t \rho + \partial_x(\rho v) - D\partial_{xx}\rho = 0, \tag{4}$$

where D is the diffusion coefficient. After making the traveling wave ansatz, assuming no flux boundary conditions, and changing to dimensionless variables, we can integrate Eq. (4) to obtain [10]

$$\rho(y) = \frac{e^{\lambda(\sigma(y)-V\mathcal{L}y)}}{\int_{-1/2}^{1/2} e^{\lambda(\sigma(y)-V\mathcal{L}y)}dy}. \tag{5}$$

Here, the density is normalized by $\bar{\rho} = \bar{\tau}/\chi$, and $\lambda = \chi\bar{\rho}/(\xi D)$ is a new parameter.

At small values of λ, the system of two equations (5), (2) has only a trivial solution $\sigma(y) = \sigma_0 = 1$ and $V = 0$. This solution becomes unstable at $\lambda_c = 1 - \omega^2/\mathcal{L}^2$, where ω is the smallest root of the algebraic equation $2\tanh(\omega/2) = \lambda_c\omega$. Through the pitchfork bifurcation shown in Fig. 2, the cell becomes polarized and starts to move [10]. As λ increases, the motors progressively concentrate at the trailing edge. For keratocytes, we use Refs. [22,25] to find that $D \sim 10^{-13}$ m^2 s^{-1} which gives $\lambda_e \sim 0.5$. We then obtain an estimate $V_e = 0.08$ μm s^{-1}, which is very close to the value measured in Ref. [5]. Interestingly, for $\mathcal{L} \sim 10$, we get $\lambda_c \sim 0.23$, which implies that keratocytes operate rather close to the bifurcation point. The proximity to *criticality* may carry considerable biological advantages; in particular, a cell can easily switch from static to motile state or change the direction of the already initiated motion.

The next step is to find the link between the value of the nondimensional parameter λ fully characterizing the transport problem and the cost parameter $\mathcal{H}^{**}$ from the optimization problem. For simplicity, we assume that the system is in contact with a thermal reservoir imposing a constant temperature T. To introduce the thermodynamic

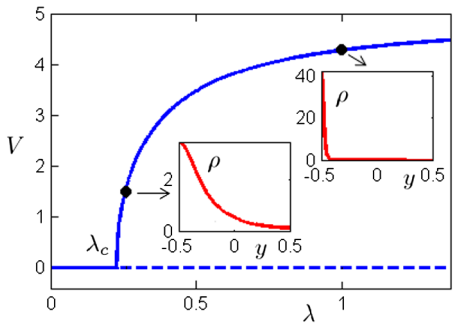

FIG. 2 (color online). Cell velocity as a function of the nondimensional parameter λ. Inserts show the density profiles for motors. The symmetric motile branch associated with negative velocities is not shown. Parameter $\mathcal{L} = 10$. Characteristic scale of velocity is $\bar{\tau}/\sqrt{\eta\xi} \sim 0.02$ μm s^{-1}

model (see Ref. [23] for more detail), we temporarily bring back the dimensional variables.

Following the general theory of active gels [15], we describe the actomyosin network as a two-phase mixture with the total mass density $\hat{\rho}(x,t)$. It is transported as a passive scalar and satisfies the conservation equation

$$\partial_t\hat{\rho} + \partial_x(\hat{\rho}v) = 0,$$

which decouples from the force balance problem due to the assumption of infinite compressibility: if the velocity field $v(y)$ is known, $\hat{\rho}(y)$ can be reconstructed by standard methods [10,13]. A comparison of the computed and the experimentally observed profiles for both $\rho(y)$ and $\hat{\rho}(y)$, see Ref. [5], show striking resemblance [23].

The total free energy of the crawling fragment can be written as

$$F = \int_{-L/2}^{L/2} \hat{\rho} f dx,$$

where $f(\phi,\zeta)$ is the energy density, which depends on the mass fraction (concentration) of motors in the mixture $\phi(x,t) = \rho/\hat{\rho}$ and on a variable $\zeta(x,t)$ characterizing the progress of a nonequilibrium chemical reaction supplying energy to the motors. We can then write

$$H = -\dot{F}, \tag{6}$$

where the dot denotes the full time derivative. To compute the right-hand side, we introduce the chemical potential of motor molecules $\mu = \partial_\phi f$ and the driving force of the reaction $A = -\partial_\zeta f > 0$, which is assumed to be fixed by an external "chemostat" [23]. We can then write

$$\dot{F} = \int_{-L/2}^{L/2} \hat{\rho}(-A\dot{\zeta} + \mu\dot{\phi})dx.$$

To show thermodynamic consistency of Eq. (4) and to derive an additional equation for the variable $\zeta(x,t)$, we observe that the dissipation rate R can be written in the form

$$R = W - \dot{F},$$

where $W = \int_{-L/2}^{L/2} \sigma\partial_x v dx$ is the external power. Assuming that there are no sources of motors, we write

$$\hat{\rho}\,\dot{\phi} = \partial_x J,$$

where J is the diffusion flux. Hence,

$$R = \int_{-L/2}^{L/2} (\sigma\partial_x v + \hat{\rho}\,\dot{\zeta}\,A + J\partial_x\mu)dx.$$

We postulate linear relations between fluxes and forces: $\sigma = l_{11}\partial_x v + l_{12}A$, $\hat{\rho}\,\dot{\zeta} = -l_{12}\partial_x v + l_{22}A$, where we

omitted the coupling between diffusion and reaction and between diffusion and viscosity.

Since motors are enzymes catalyzing the Adenosine triphosphate (ATP) hydrolysis reaction, we must deviate from the quasiequilibrium scheme and consider the coefficients l_{12} and l_{22} as functions of the motor density ρ; in view of our postulate $\tau = l_{12}A = \chi\rho$, these functions must be linear. Other dissipative mechanisms are assumed to be Onsagerian, in particular, $l_{11} = \eta$. To compute the diffusion coefficient in Eq. (4), we notice that for dilute mixtures $\partial_\phi \mu = k_B T/\phi$, where k_B is Boltzmann's constant. If we make additional assumptions that the variation of the total density is small $\partial_x \rho/\rho \gg \partial_x \hat{\rho}/\hat{\rho}$ and the diffusion coefficient is concentration independent, we recover Eq. (4) with $D = l_{33} k_B T/\bar{\rho}$, where l_{33} is the mobility per unit volume. These assumptions clearly fail near the singularities of ρ where the theory has to be appropriately modified.

An important outcome of our constitutive assumptions is an equation governing the reaction progress

$$\dot{\zeta} = \phi\left(bA - \frac{\chi}{A}\partial_x v\right), \tag{7}$$

where in view of the linearity assumption for l_{22}, $b = l_{22}/\rho$ is a constant. Since the value of A is controlled externally, Eq. (7) decouples from the rest of the system with ζ easily recoverable once the fields v and ϕ are known.

We have now specified the force generation mechanism and can use Eq. (6) to obtain an explicit expression for the cost function H. First, using the force balance equation, we write the mechanical cost function in the form

$$H^* = \int_{-L/2}^{L/2} [\xi v^2 + \eta(\partial_x v)^2] dx \geq 0,$$

where the two entries characterize contributions due to friction and viscosity. The nonmechanical cost function can be written as

$$H^{**} = \int_{-L/2}^{L/2} \left[b\rho A^2 + \frac{D k_B T}{\bar{\rho}}(\partial_x \rho)^2\right] dx \geq 0.$$

Here, the two terms are the cost of keeping the chemical reaction out of equilibrium and the cost of supporting concentration gradients. In agreement with the fact that the motion is driven exclusively by the chemostat, we obtain for the physical solution that both $H^* \to 0$ and $H^{**} \to 0$ as $A \to 0$ [23].

To make comparison with the optimization model, we need to compute the dimensionless quantity

$$\mathcal{H}^{**} = \mathcal{M}\mathcal{L} + \frac{\mathcal{E}}{\lambda \mathcal{L}} \int_{-1/2}^{1/2} (\partial_y \rho)^2 dy, \tag{8}$$

where we introduced two new parameters: $\mathcal{M} = \eta b A^2/(\bar{\rho}\chi^2)$ and $\mathcal{E} = k_B T/\chi$. If motors operate in stall conditions and form bipolar contractile units with size d, the produced force is $p \sim 2\chi/d$. For myosin II, we have $d \sim 0.15$ μm and $p \sim 1.5$ pN [26], which gives $\chi \sim 1.1 \times 10^{-19}$ J and using $k_B T \sim 4.3 \times 10^{-21}$ J, we obtain $\mathcal{E} \sim 0.04$. Notice also that bA^2 is the free energy consumption rate per motor and, therefore, that it is equal to kA, where k is the rate of ATP turnover per motor. Since $A \sim 25 k_B T$ and $k \sim 25$ s^{-1} [26], we obtain $\mathcal{M} \sim 0.05$.

We can now fix the parameters $\mathcal{E}, \mathcal{M}$ and compare physical and optimal efficiencies at different values of the remaining parameter λ. The efficiency in the physical model is $\Lambda_{\rm ph}(\rho_{\rm ph}, \mathcal{H}^{**})$, where $\rho_{\rm ph}(y, \lambda)$ is the solution of Eq. (4), and $\mathcal{H}^{**}(\lambda)$ is taken from Eq. (8). The ensuing function $\Lambda_{\rm ph}(\lambda)$ is to be compared with the optimal efficiency $\Lambda_{\rm op}(\lambda) = \Lambda_{\rm op}(\rho_{\rm op}, \mathcal{H}^{**})$, where $\rho_{\rm op}(y, \mathcal{H}^{**})$ is the solution of the optimization problem, and $\mathcal{H}^{**}(\lambda)$ is the same as above.

The results of the comparison are summarized in Fig. 3. The function $\Lambda_{\rm ph}(\lambda)$ displays a single maximum at $\lambda_o \sim 0.24$. For all $\lambda \geq \lambda_o$, the physical model remains close to the optimal one, which is crucial, since at $\lambda \to \infty$, the rate of energy consumption diverges $\mathcal{H}^* \sim \mathcal{L}^3\lambda/3$, $\mathcal{H}^{**} \sim \mathcal{E}\mathcal{L}^5\lambda^2/15$. In this (high-velocity) limit, both physical and optimization problems generate the same profiles with motors infinitely localized at the trailing edge of the moving cell. The robust optimality in the range $V \geq V_0(\lambda_o) \sim 1.1$ is illustrated further in Fig. 4, where we show the ratio $r = \Lambda_{\rm ph}/\Lambda_{\rm op} \leq 1$ as a function of V/V^∞. The presence of a quasiplateau on this graph in the biologically relevant range of velocities [5] and the fact that in this range the physical and the optimal efficiencies are close suggest that the system is tuned to optimality. In the immediate vicinity of the motility initiation point $V = 0$ where $\lambda \sim \lambda_c$, the asymptotic solutions in the two models have the same general structure $\rho(y) - 1 \sim (\lambda - \lambda_c)^\kappa f(y)$; however, since $\kappa_{\rm ph} = 1/2$ and $\kappa_{\rm op} = 0$, the propulsion machinery operates suboptimally in this regime, and this

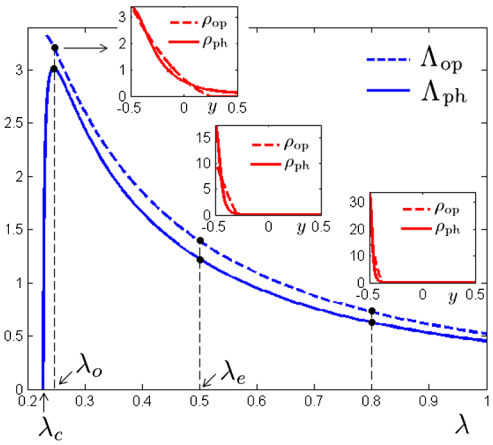

FIG. 3 (color online). Physical and optimal efficiencies as functions of the dimensionless parameter λ. Inserts compare optimal and physical distributions of motors. Parameters: $\mathcal{L} = 10$, $\mathcal{M} = 0.05$, and $\mathcal{E} = 0.04$.

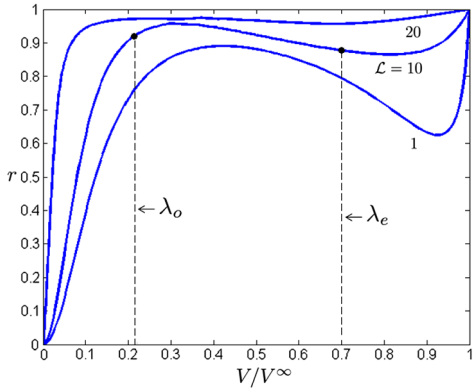

FIG. 4 (color online). Ratio of physical and optimal efficiencies as a function of cell velocity. Indicated are the low bound of the regimes of near-optimal performance $V_o(\lambda_o)$ and the experimentally observed regime $V_e(\lambda_e)$. The symmetric branch associated with negative velocities is not shown. Parameters are $\mathcal{L} = 1, 10, 20$, $\mathcal{M} = 0.05$, and $\mathcal{E} = 0.04$.

may explain why small velocities have not been observed in experiments.

As Fig. 4 shows, the increase of $\mathcal{L}$ progressively broadens the optimality plateau; in particular, in the inviscid limit, all dynamic regimes are exactly optimal. On the other hand, if we use a lower value of the friction coefficient from Ref. [22] corresponding to the smaller value $\mathcal{L} = 0.44$, we obtain an efficiency-velocity relation which is indistinguishable from the saturation limit shown in Fig. 4 for $\mathcal{L} = 1$. In all these cases, the physical regime remains close to optimality. An additional study of robustness of our predictions with respect to parameters $\mathcal{M}$ and $\mathcal{E}$ is presented in Ref. [23].

In conclusion, we have shown that in contraction-dominated crawling, the optimal trade-off between Stokes performance and the metabolic cost is achieved by a rather sharp localization of contractile units at the trailing edge of the moving cell. A simple advection-diffusion model of motor redistribution based on the active gel theory performs almost optimally in the range of parameters suggested by *in vivo* measurements. The fact that the near-optimal behavior is robust and extends into the domain of parameters where suboptimality would be particularly costly, suggests that contraction-dominated crawling presents an example of a remarkably perfected biological mechanism.

The authors thank F. Alouges, G. Geymonat, and T. Putelat for helpful discussions. P. R. thanks the Fondation Pierre-Gilles de Gennes for generous support.

[1] D. Hu and D. Cai, Phys. Rev. Lett. **111**, 138701 (2013); T. Takahashi, *Microcirculation in Fractal Branching Networks* (Springer, New York, 2013), pp. 1–24.
[2] D. Mortimer, P. Dayan, K. Burrage, and G. J. Goodhill, Neural Comput. **23**, 336 (2011).
[3] V. Chubukov, I. A. Zuleta, and H. Li, Proc. Natl. Acad. Sci. U.S.A. **109**, 5127 (2012).
[4] P. Szekely, H. Sheftel, A. Mayo, and U. Alon, PLoS Comput. Biol. **9**, e1003163 (2013).
[5] A. Verkhovsky, T. Svitkina, and G. Borisy, Curr. Biol. **9**, 11 (1999).
[6] G. Taylor, Proc. R. Soc. A **209**, 447 (1951).
[7] E. Lauga and T. R. Powers, Rep. Prog. Phys. **72**, 096601 (2009).
[8] F. Alouges, A. DeSimone, and A. Lefebvre, J. Nonlinear Sci. **18**, 277 (2008).
[9] A. DeSimone and A. Tatone, Eur. Phys. J. E **35**, 1 (2012).
[10] P. Recho, T. Putelat, and L. Truskinovsky, Phys. Rev. Lett. **111**, 108102 (2013).
[11] P. T. Yam, C. A. Wilson, L. Ji, B. Hebert, E. L. Barnhart, N. A. Dye, P. W. Wiseman, G. Danuser, and J. A. Theriot, J. Cell Biol. **178**, 1207 (2007).
[12] A. E. Carlsson, New J. Phys. **13**, 073009 (2011).
[13] P. Recho and L. Truskinovsky, Phys. Rev. E **87**, 022720 (2013).
[14] B. Rubinstein, M. F. Fournier, K. Jacobson, A. B. Verkhovsky, and A. Mogilner, Biophys. J. **97**, 1853 (2009); A. Jilkine and L. Edelstein-Keshet, PLoS Comput. Biol. **7**, e1001121 (2011); K. Doubrovinski and K. Kruse, Phys. Rev. Lett. **107**, 258103 (2011); N. Hodge and P. Papadopoulos, J. Math. Biol. **64**, 1253 (2012); E. Tjhung, D. Marenduzzo, and M. E. Cates, Proc. Natl. Acad. Sci. U.S.A. **109**, 12381 (2012); F. Ziebert and I. S. Aranson, PLoS One **8**, e64511 (2013); A. Callan-Jones and R. Voituriez, New J. Phys. **15**, 025022 (2013); B. A. Camley, Y. Zhao, B. Li, H. Levine, and W.-J. Rappel, Phys. Rev. Lett. **111**, 158102 (2013).
[15] K. Kruse, J. Joanny, F. Julicher, J. Prost, and K. Sekimoto, Eur. Phys. J. E **16**, 5 (2005).
[16] F. Julicher, K. Kruse, J. Prost, and J.-F. Joanny, Phys. Rep. **449**, 3 (2007).
[17] M. Marchetti, J. Joanny, S. Ramaswamy, T. Liverpool, J. Prost, M. Rao, and R. A. Simha, Rev. Mod. Phys. **85**, 1143 (2013).
[18] M. J. Lighthill, Commun. Pure Appl. Math. **5**, 109 (1952).
[19] A. V. Hill, Proc. R. Soc. B **126**, 136 (1938).
[20] E. M. Purcell, Am. J. Phys. **45**, 3 (1977).
[21] U. S. Schwarz and S. A. Safran, Phys. Rev. Lett. **88**, 048102 (2002).
[22] E. L. Barnhart, K.-C. Lee, K. Keren, A. Mogilner, and J. A. Theriot, PLoS Biol. **9**, e1001059 (2011).
[23] See Supplemental Material at http://link.aps.org/supplemental/10.1103/PhysRevLett.112.218101 for mathematical solution of the optimization problem, detailed thermodynamical derivation of the physical model, comparison with experiments [5] and the sensitivity study of efficiency with the remaining parameters.
[24] J. S. Bois, F. Jülicher, and S. W. Grill, Phys. Rev. Lett. **106**, 028103 (2011).
[25] T. Luo, K. Mohan, V. Srivastava, Y. Ren, P. A. Iglesias, and D. N. Robinson, Biophys. J. **102**, 238 (2012).
[26] J. Howard, *Mechanics of Motor Proteins and the Cytoskeleton* (Sinauer Associates, Sunderland, MA, 2001).